

# Manipulation of Majorana fermion, Andreev reflection and Josephson current on topological insulators

Yukio Tanaka<sup>1</sup>, Takehito Yokoyama<sup>2</sup> and Naoto Nagaosa<sup>2,3</sup>

<sup>1</sup>Department of Applied Physics, Nagoya University, Nagoya, 464-8603, Japan

<sup>2</sup>Department of Applied Physics, University of Tokyo, Tokyo 113-8656, Japan

<sup>3</sup> Cross Correlated Materials Research Group (CMRG), ASI, RIKEN, WAKO 351-0198, Japan

(Dated: October 24, 2018)

We study theoretically charge transport properties of normal metal (N) / ferromagnet insulator (FI) / superconductor (S) junction and S/FI/S junction formed on the surface of three-dimensional topological insulator (TI), where chiral Majorana mode (CMM) exists at FI/S interface. We find that CMM generated in N/FI/S and S/FI/S junctions are very sensitively controlled by the direction of the magnetization  $\mathbf{m}$  in FI region. Especially, the current-phase relation of Josephson current in S/FI/S junctions has a phase shift neither 0 nor  $\pi$ , which can be tuned continuously by the component of  $\mathbf{m}$  perpendicular to the interface.

PACS numbers: 74.45.+c,71.10.Pm,74.90.+n

The class of time-reversal (TR) symmetric insulators with the nontrivial topological properties has been proposed theoretically and discovered experimentally [1, 2, 3]. The hallmark of this insulator, i.e., topological insulator (TI), is the edge or surface channels, while the bulk states are gapped and inert for the low energy phenomena. In the two-dimensional (2D) case, there appears the helical modes at the edge of the sample, i.e., the pair of one-dimensional modes connected by the time-reversal symmetry and propagating in the opposite directions for opposite pseudo-spins [2]. This is analogous to the chiral edge modes in the quantum Hall systems [4]. Therefore, the TI in 2D case can be regarded as the two copies of the quantum Hall systems for up and down pseudo-spins [5], and is often called the quantum spin Hall system. In three-dimensional (3D) case, there are two class of TI, i.e., weak TI (WTI) and strong TI (STI), corresponding to the even (WTI) and odd (STI) number of the chiral Dirac fermions on the surface [6]. Since the even number of Dirac fermions can be paired to open the gap, those in WTI is fragile against the disorder and/or the interactions while they are robust in STI. The 2D quantum spin Hall system is adiabatically continued to the WTI when the weak interlayer coupling is tuned, while the STI has no analogue to the quantum Hall system, and is a genuine new state of matter.

The 2D chiral Dirac fermion on the surface of STI is protected by the bulk gap and its topological property. Therefore, it offers an interesting system to look for the 2D superconductivity with the Cooper pairs mediated by the bosonic excitations, e.g., phonons and excitons, in the STI. Fu and Kane studied the superconductivity induced by the proximity effect to the surface of STI [7]. Considering the interface between the ferromagnetic insulator (FI) and conventional superconductor (S), they predicted the appearance of the chiral Majorana state as an Andreev bound state [7]. We call this chiral Majorana mode (CMM), which has a dispersion along the interface while it is confined along the direction perpendicular to the interface. Detecting the Majorana fermions in terms

of the interferometry has been proposed also [8, 9].

The presence of CMM is predicted in the  $p_x + ip_y$  chiral superconductors [10], e.g.,  $\text{Sr}_2\text{RuO}_4$ . However the control of the chiral domains and manipulation of the edge channels are experimentally difficult [11]. In addition, the  $p_x + ip_y$  superconductivity is very fragile against the disorder. Also, the CMM in the  $^3\text{He}$  and cold atoms have been studied theoretically [12], but they are neutral systems and charge transport is missing there. Therefore, the present system offers unique opportunity to study the quantum charge transport specific to CMM and its control, which is more promising to be realized experimentally. However, its theoretical studies have been limited focusing on the detection of the Majorana fermion itself [8, 9, 13].

In this paper, we study the manipulation of the quantum transport properties associated with Majorana fermions at the interface of the superconductor (S) and ferromagnetic insulator (FI) generated on the surface on TI. Hereafter, since we concentrate on the STI, we denote TI instead of STI for simplicity. We show that the direction of the magnetization  $\mathbf{m}$  can be used to control the Andreev reflection and Josephson current via the CMM generated in N/FI/S and S/FI/S junctions, offering a unique method for superconducting spintronics.

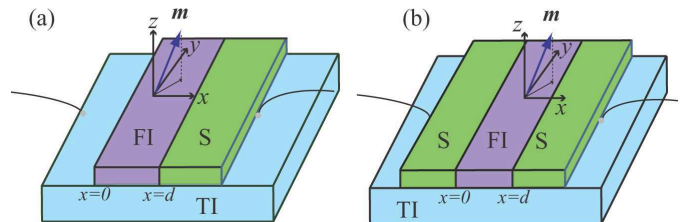


FIG. 1: Schematic illustration of the junction. (a) Normal metal (N) / Ferromagnetic insulator (FI) / Superconductor (S) junction and (b) S/FI/S junction formed on the surface of 3D topological insulator (TI). The current is flowing on the surface of TI.

We consider FI/S and S/FI/S structures formed on the surface of 3D topological insulators as shown in Fig. 1. We concentrate on the situation that TI below FI becomes ferromagnetic insulator due to the exchange coupling. Since surface state of TI is metallic, we can regard the configuration shown in Fig. 1(a) as normal metal (N)/FI/S junction with  $N(x < 0)$ ,  $FI(0 < x < d)$ , and  $S(x > d)$ . We also consider S/FI/S junction as shown in Fig. 1(b) with  $S(x < 0)$ ,  $FI(0 < x < d)$ , and  $S(x > d)$ . The interfaces N(S)/FI and FI/S locate at  $x = 0$  and  $x = d$ , respectively. We assume that the chemical potential in N and S are equal to each other.

The Hamiltonian of the surface state on TI is given by

$$\hat{H}_S = \begin{pmatrix} \hat{H}(\mathbf{k}) + \hat{M} & \hat{\Delta} \\ -\hat{\Delta}^* & -\hat{H}^*(-\mathbf{k}) - \hat{M}^* \end{pmatrix} \quad (1)$$

with  $\hat{H}(\mathbf{k}) = v_F(\hat{\sigma}_x k_x + \hat{\sigma}_y k_y) - \mu[\Theta(-x) + \Theta(x - d)]$ , and  $\hat{M} = \mathbf{m} \cdot \hat{\boldsymbol{\sigma}}\Theta(d - x)\Theta(x)$  with  $\mathbf{m} \cdot \hat{\boldsymbol{\sigma}} = m_x \hat{\sigma}_x + m_y \hat{\sigma}_y + m_z \hat{\sigma}_z$ . Here,  $\mu$ ,  $\hat{\boldsymbol{\sigma}}$ ,  $v_F$ ,  $\mathbf{m}$  denote chemical potential, Pauli matrices, velocity, and magnetization (times the exchange coupling constant which we assume to be 1), respectively [7]. Note that  $\mathbf{m}$  enters as an effective vector potential  $\mathbf{A}$  of the electromagnetic field. The pairing symmetry of superconductor is assumed to be  $s$ -wave and  $\hat{\Delta}$  is given as  $\hat{\Delta} = i\hat{\sigma}_y \Delta \Theta(x - d)$  and  $\hat{\Delta} = i\hat{\sigma}_y [\Delta \Theta(x - d) + \Delta \Theta(-x) \exp(i\varphi)]$  for N/TI/S and S/TI/S junctions, respectively, where  $\varphi$  denotes the macroscopic phase difference between left and right superconductor. In general, the magnitude of  $\Delta$  is smaller than that of the bulk energy gap of superconductor deposited on TI due to the nonideal S/TI interface [14].

First, let us consider N/FI/S junction (Fig. 1(a)). A wave function of an electron injected from N with an injection angle  $\theta$  is given as  $\Psi_T = \exp(ik_y y)[\Psi_N(x)\Theta(-x) + \Psi_{FI}(x)\Theta(x)\Theta(d - x) + \Psi_S^R(x)\Theta(x - d)]$ , where  $k_y = k_F \sin \theta$  is the momentum parallel to the interface with  $v_F k_F = \mu$ .  $\Psi_N(x)$ ,  $\Psi_{FI}(x)$  and  $\Psi_S^R(x)$  are given by

$$\Psi_N(x) = [(\Psi_{in} + a\Psi_{hr}) \exp(ik_x x) + b\Psi_{er} \exp(-ik_x x)] \quad (2)$$

$$\Psi_{FI}(x) = [\Psi_{e1} \exp(-\tilde{\kappa}x) + \Psi_{e2} \exp(\tilde{\kappa}^*x) + \Psi_{h1} \exp(\tilde{\kappa}x) + \Psi_{h2} \exp(-\tilde{\kappa}^*x)] \quad (3)$$

$$\Psi_S^R(x) = [\Psi_{et} \exp(ik_x x) + \Psi_{ht} \exp(-ik_x x)] \quad (4)$$

with  $k_x = \sqrt{(\mu/v_F)^2 - k_y^2}$ ,  $\tilde{\kappa}_x = \kappa_x + im_x/v_F$ , and  $\kappa_x = \sqrt{m_z^2 + (v_F k_y + m_y)^2}/v_F$ . The four component wave functions  $\psi_{in}$ ,  $\psi_{hr}$  and  $\psi_{er}$  are given by  ${}^T \psi_{in} = (1, \exp(i\theta), 0, 0)$ ,  ${}^T \psi_{hr} = (0, 0, 1, -\exp(i\theta))$ ,  ${}^T \psi_{er} = (1, -\exp(-i\theta), 0, 0)$ , with  $\exp(i\theta) = (k_x + ik_y)/k_F$ . Other wave functions  $\psi_{e1}$ ,  $\psi_{e2}$ ,  $\psi_{h1}$ ,  $\psi_{h2}$ ,  $\psi_{et}$ , and  $\psi_{ht}$  are obtained by solving eq. (1) in a similar way.

The coefficients of Andreev reflection  $a$  and normal reflection  $b$  are obtained by imposing the boundary condition  $\Psi_N(x = 0) = \Psi_{FI}(x = 0)$ , and  $\Psi_{FI}(x = d) = \Psi_S^R(x = d)$ . Then, the angle resolved tunneling conductance for injection angle  $\theta$  is obtained by standard way

as  $\sigma_S(\theta) = 1 + |a|^2 - |b|^2$ . The normalized angle averaged tunneling conductance  $\sigma$  by its value in the normal state is given by [15]

$$\sigma = \frac{\int_{-\pi/2}^{\pi/2} \sigma_S(\theta) \cos \theta d\theta}{\int_{-\pi/2}^{\pi/2} \sigma_N \cos \theta d\theta} \quad (5)$$

$$\sigma_S(\theta) = \frac{\sigma_N [1 + \sigma_N |\Gamma|^2 - (1 - \sigma_N) |\Gamma|^4]}{|1 + (1 - \sigma_N) \exp(i\gamma) \Gamma^2|^2} \quad (6)$$

with  $\exp(i\gamma) = [m_z \cos \theta + i(\mu \sin \theta + m_y)]/[m_z \cos \theta - i(\mu \sin \theta + m_y)]$  and  $\Gamma = \Delta/(E + \sqrt{E^2 - \Delta^2})$ .  $\sigma_N$  denotes the transparency of the junction in the normal state given by  $\sigma_N = 1/(\cosh^2(\kappa_x d) + \tan^2 \theta \sinh^2(\kappa_x d) k_y^2/\kappa_x^2)$ . For  $\sigma_N \rightarrow 0$ , the denominator of  $\sigma_S(\theta)$  becomes zero at  $E = E_b$

$$E_b = -\frac{\Delta(\mu \sin \theta + m_y) \text{sgn}(m_z)}{\sqrt{(\mu \sin \theta + m_y)^2 + \cos^2 \theta m_z^2}}. \quad (7)$$

This condition coincides with the formation of CMM at the FI/S interface with semi-infinite. CMM and Andreev reflection are strongly related to each other and  $|a| = 1$  is satisfied at  $E = E_b$  independent of  $\sigma_N$ . It is noted that the sign of  $E_b$  is changed by reversing the direction of magnetization  $m_z$ .  $E_b$ ,  $\sigma_S(\theta)$  and  $\sigma$  are independent of  $m_x$ . As a special limit of  $m_z = \mu$  and  $m_y = 0$ , this formula includes the case of chiral  $p_x + i \text{sgn}(-m_z) p_y$ -wave superconductor where  $E_b$  is reduced to be  $E_b = -\Delta \sin \theta \text{sgn}(m_z)$  [16] although the given pair potential is full gap  $s$ -wave. It is remarkable that the sign of  $m_z$  corresponds to the chirality of the CMM, which can be controlled by the direction of magnetization of FI. Here, we focus on how the above CMM influences the bias voltage  $V$  dependence of conductance in N/FI/S junctions with  $E = eV$ . As shown in Fig. 2, the resulting  $\sigma$  has a zero bias conductance peak (ZBCP) originating from the peak of  $\sigma_S(\theta)$  at  $E = E_b$ . As seen from the left panel of Fig. 2, the slope of the curve of  $E_b$  around  $E_b = 0$  ( $\theta = 0$ ) becomes gradual with the decrease of  $\mu/m_z$ . Then, the contribution around  $\theta = 0$  becomes significant in the integral of numerator in eq. (5) and the resulting height of the ZBCP is enhanced with the decrease of the magnitude of  $\mu/m_z$  as shown in the right panel.

The presence of  $m_y$  changes  $E_b$  drastically since  $E_b(\theta) = -E_b(-\theta)$  does not hold any more. As shown in the left panel of Fig. 3, in the presence of  $m_y$ ,  $E_b$  does not become zero any more for  $\theta = 0$ . For  $m_y/m_z = 0.4$ , the domain of  $\theta$  with negative  $E_b$  is larger than that of positive one. The resulting  $\sigma$  has a peak at negative bias voltage as seen from curve  $b$  in the right panel of Fig. 3. On the other hand, for  $m_y/m_z = -0.4$ , the domain of  $\theta$  with positive  $E_b$  is larger than that of negative one as seen from curve  $c$  in the left panel. Then the resulting  $\sigma$  has a peak at positive bias voltage as seen from curve  $c$  in the right panel of Fig. 3. As shown above, CMM, Andreev reflection and resulting  $\sigma_S(\theta)$  are critically controlled by  $\mathbf{m}$ . The present CMM is significantly different

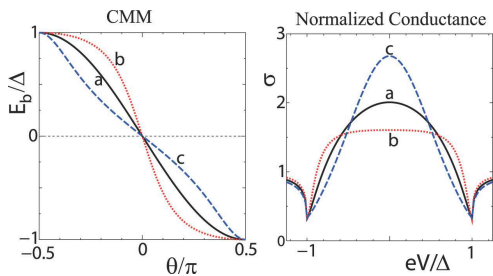


FIG. 2: (Color online) Left Panel: Chiral Majorana mode (CMM) energy level  $E_b$  as a function of the incident angle  $\theta$ . Right Panel: Normalized tunneling conductance  $\sigma$  in N/FI/S junctions.  $m_z d/v_F = 1$  and  $m_y/m_z = 0$ . a:  $\mu/m_z = 1$ , b:  $\mu/m_z = 2$  and c:  $\mu/m_z = 0.5$ .

from that in the non-centrosymmetric superconductor, where CMM appears as helical edge modes [17]. In the present case, one of the spin-split bands is missing compared with the non-centrosymmetric superconductors.

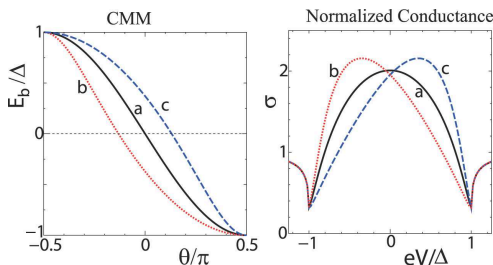


FIG. 3: (Color online) Left Panel: CMM energy level  $E_b$ . Right Panel:  $\sigma$  in N/FI/S junctions.  $m_z d/v_F = 1$  and  $\mu/m_z = 1$ . a:  $m_y/m_z = 0$ , b:  $m_y/m_z = 0.4$  and c:  $m_y/m_z = -0.4$ .

Next, we focus on the Josephson current in S/FI/S junction (Fig. 1(b)). Since the magnitude of the pair potential of the left and right superconductors are equal to each other, it is possible to evaluate the Josephson current by using the CMMs formed in S/FI/S junctions [18]. The CMMs can be obtained as in the case of N/FI/S junction with wave functions of Eq. (1) under a proper boundary condition. The resulting Josephson current  $I$  can be obtained as

$$I = \frac{2e}{\hbar} \frac{\partial F}{\partial \varphi}, \quad F = -k_B T \sum_{\mathbf{k}} \log[2 \cosh(\frac{E_J}{2k_B T})], \quad (8)$$

$$E_J = \sqrt{\sigma_N \cos^2(\varphi/2 - \delta) + (1 - \sigma_N)(E_b/\Delta)^2} \Delta \quad (9)$$

with  $\delta = m_x d/v_F$  and temperature  $T$ . The appearance of  $\delta$  in the current-phase relation stems from the fact that  $\tilde{\kappa}_x$  in eq. (3) becomes complex number in the presence of  $m_x$ . The position of the present CMMs in S/FI/S junctions is given by  $\bar{E}_b = \pm E_J$ . The expression of  $\bar{E}_b$  can be explained by the hybridization of two CMM formed at the left S/FI interface and right FI/S interface. The formula

of  $\bar{E}_b$  [eq. (9)] is very general including several preexisting cases. As a special limit with  $E_b = \Delta$ , and  $m_x = 0$ ,  $\bar{E}_b$  is reduced to  $\bar{E}_b = \pm \sqrt{\cos^2(\varphi/2) + (1 - \sigma_N) \sin^2(\varphi/2)} \Delta$ , which corresponds to the Andreev bound state in conventional S/non-magnetic insulator (NI)/S junction [19]. If we choose  $E_b = 0$ , and  $m_x = 0$ , the bound state formula in  $d_{xy}(p_x)$ -wave /NI/ $d_{xy}(p_x)$ -wave junction is reproduced [19]. To understand the  $\theta$  and  $\varphi$  dependence of  $\bar{E}_b$  ( $E_J$ ) more intuitively, we plot  $E_J$  (absolute value of  $\bar{E}_b$ ) in Fig. 4.  $E_J$  is an even function of  $\theta$  for any  $m_x$ . For  $m_x = 0$ ,  $E_J$  is symmetric with respect to  $\varphi = 0$  (Fig. 4(a)). However, for  $m_x \neq 0$ , the resulting  $E_J$  is no more symmetric around  $\varphi = 0$  as shown in Figs. 4(b) and 4(c). This fact seriously influences the Josephson current  $I$  given by

$$eIR_N = \frac{\sin(\varphi - 2\delta) \int_{-\pi/2}^{\pi/2} d\theta \frac{\pi \Delta^2 \tanh(E_J/2k_B T) \sigma_N \cos \theta}{2E_J}}{\int_{-\pi/2}^{\pi/2} d\theta \sigma_N \cos \theta} \quad (10)$$

with resistance in the normal state  $R_N$ .

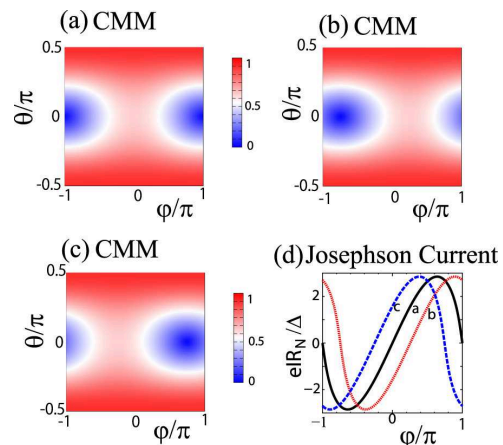


FIG. 4: (Color online) Contour plot of CMM energy level  $E_J$  as a function of  $\theta$  and  $\varphi$  for (a)  $m_x = 0$ , (b)  $m_x = 0.4m_z$ , (c)  $m_x = -0.4m_z$ . The resulting Josephson current in S/FI/S junctions is plotted in (d) with a:  $m_x/m_z = 1$ , b:  $m_x/m_z = 0.4$  and c:  $m_x/m_z = -0.4$ . In all panels, we choose  $m_z d/v_F = 1$ ,  $\mu/m_z = 1$  and  $m_y/m_z = 0$ .  $T = 0.05T_C$  with transition temperature  $T_C$ .

Differently from  $\sigma$  for the Andreev reflection,  $I$  is almost independent of  $m_y$  because the contributions to the change in  $I$  almost cancel between the two CMMs with opposite chiralities. On the other hand,  $m_x$  seriously influences  $I$  as the effective vector potential which directly enters into the phase of the Josephson coupling  $\varphi$ . Here, the absence of the small factor of  $e/c$ , which reduces the coupling to the magnetic field, makes the tuning of the current-phase relation much easier. Reflecting the  $\varphi$  dependence of  $E_J$ , the resulting  $I$  becomes zero at neither  $\varphi = 0$  nor  $\varphi = \pm\pi$  (curves b and c in Fig. 4(d)) due to the presence of the phase shift  $2\delta$ . Up to now, there have been many studies about Josephson

current in ferromagnet junctions [20], where the value of phase shift becomes neither 0 nor  $\pi$  in usual cases. The intermediate phase shift has been predicted in a few cases even in the absence of Majorana Fermion, i) spin-singlet  $s$ -wave / spin-triplet superconductor junction [21], ii) even-frequency / odd-frequency superconductor junction [22], and iii) ferromagnet junction with spin-singlet  $s$ -wave superconductor in the presence of the spin-flip scattering or spin-orbit coupling [23, 24]. It is remarkable that this anomalous current-phase relation appears simply controlling one magnetization vector without using unconventional pairing in the present model. It is also noted that the resulting current-phase relation can be continuously tuned by the change of  $m_x$  similar to the control of the magnetization vectors at the interfaces of ferromagnet junction [23]. We hope this anomalous current-phase relation will be detected experimentally in SQUID.

In conclusion, we have studied the charge transport properties of normal metal (N) / ferromagnet insulator

(FI) / superconductor (S) junction and S/FI/S junction formed on the surface of three-dimensional (3D) topological insulator, where chiral Majorana mode (CMM) exists at FI/S interface. We have found that CMM generated in N/FI/S and S/FI/S junctions are controlled by the direction of the magnetization  $\mathbf{m}$  in FI region very sensitively. Since metallic surface state of 3D topological insulator has been observed experimentally, our proposed structure will be accessible in the near future [25]. Our results give a guide to innovate novel direction of superconducting spintronics.

Note added: After a submission of this paper, a realization of the Majorana fermion in superconductor / semiconductor heterostructure has been predicted in the presence of interplay of spin-orbit coupling and exchange field [26].

This work is partly supported by the Grant-in-Aids from under the Grant No. 20654030, No. 19048015 and No. 19048008 from MEXT, Japan, and NTT basic research laboratories. T.Y. acknowledges support by JSPS.

- 
- [1] C. L. Kane and E. J. Mele, Phys. Rev. Lett. **95**, 146802 (2005); C. L. Kane and E. J. Mele, Phys. Rev. Lett. **95**, 226801 (2005); L. Fu and C. L. Kane, Phys. Rev. B **74**, 195312 (2006)
- [2] B. A. Bernevig, and S. C. Zhang, Phys. Rev. Lett. **96**, 106802 (2006); B. A. Bernevig, T. L. Hughes, and S. C. Zhang, Science **314**, 1757 (2006).
- [3] M. König, *et al.* Science, **318**, 766 (2007); M. König, *et al.* J. Phys. Soc. Jpn. **77**, 031007 (2008).
- [4] X.G. Wen, *Quantum Field Theory of Many-body Systems: From the Origin of Sound to an Origin of Light and Electrons*, (Oxford Graduate Texts ) (2004).
- [5] M. Onoda and N. Nagaosa, Phys. Rev. Lett. **95**, 106601 (2005).
- [6] Liang Fu, C. L. Kane, and E. J. Mele, Phys. Rev. Lett. **98**, 106803 (2007); L. Fu and C. L. Kane, Phys. Rev. B **76**, 045302 (2007); J. E. Moore and L. Balents, Phys. Rev. B **75**, 121306(R) (2007).
- [7] L. Fu and C. L. Kane, Phys. Rev. Lett. **100**, 096407 (2008).
- [8] L. Fu and C. L. Kane, Phys. Rev. Lett. **102**, 216403 (2009).
- [9] A. R. Akhmerov, J. Nilsson, and C.W.J. Beenakker, Phys. Rev. Lett. **102**, 216404 (2009).
- [10] N. Read and D. Green, Phys. Rev. B **61**, 10267 (2000); D. A. Ivanov, Phys. Rev. Lett. **86**, 268 (2001).
- [11] A. P. Mackenzie and Y. Maeno, Rev. Mod. Phys. **75**, (2003) 657; H. Kambara, *et al.*, Phys. Rev. Lett. **101**, 267003 (2008).
- [12] G.E. Volovik, *The Universe in a Helium Droplet*, Clarendon Press, Oxford (2003); Y. Tsutsumi, *et al.*, Phys. Rev. Lett. **101**, 135302 (2008); S. Tewari, *et al.*, Phys. Rev. Lett. **98**, 010506 (2007); M. Sato, Y. Takahashi, S. Fujimoto, Phys. Rev. Lett. **103**, 020401 (2009); T. Mizushima, M. Ichioka, and K. Machida, Phys. Rev. Lett. **101**, 150409 (2008).
- [13] J. Nilsson, A. R. Akhmerov, and C.W. J. Beenakker, Phys. Rev. Lett. **101**, 120403 (2008).
- [14] G. Fagas, *et al.*, Phys. Rev. B **71** 224510 (2005).
- [15] C. Bruder, Phys. Rev. B **41**, 4017 (1990); Y. Tanaka and S. Kashiwaya, Phys. Rev. Lett. **74**, 3451 (1995).
- [16] M. Yamashiro, Y. Tanaka, and S. Kashiwaya, Phys. Rev. B **56**, 7847 (1997); C. Honerkamp and M. Sigrist, J. Low Temp. Phys. **111**, 895 (1998); H.J. Kwon, K. Sengupta, and V.M. Yakovenko, Eur. Phys. J. B **37**, 349 (2004).
- [17] Y. Tanaka, *et al.*, Phys. Rev. B **79**, 060505(R) (2009); M. Sato and S. Fujimoto, Phys. Rev. B **79**, 094504 (2009).
- [18] C.W.J. Beenakker, Phys. Rev. Lett. **67**, 3836 (1991).
- [19] S. Kashiwaya and Y. Tanaka, Rep. Prog. Phys. **63**, 1641 (2000); A.A. Golubov, M. Yu. Kupriyanov and E. Il'ichev, Rev. Mod. Phys. **76**, 412 (2004).
- [20] A. I. Buzdin, Rev. Mod. Phys. **77**, 935 (2005); F. S. Bergeret, A. F. Volkov, and K. B. Efetov, Rev. Mod. Phys. **77**, 1321 (2005).
- [21] Y. Asano, *et al.*, Phys. Rev. B **67**, 184505 (2003).
- [22] Y. Tanaka, *et al.*, Phys. Rev. Lett. **99**, 037005 (2007).
- [23] R. Grein, *et al.*, Phys. Rev. Lett. **102**, 227005 (2009); M. Eschrig, *et al.*, J. Low Temp. Phys. **147**, 457 (2007); M. Eschrig and T. Löfwander, Nature Physics **4**, 138 (2008); Y. Asano, *et al.*, Phys. Rev. B **76**, 224525 (2007); V. Braude and Yu. V. Nazarov, Phys. Rev. Lett. **98** 077003 (2007).
- [24] A. Buzdin, Phys. Rev. Lett. **101**, 107005 (2008); F. Konschelle and A. Buzdin, Phys. Rev. Lett. **102**, 017001, (2009).
- [25] D. Hsieh, *et al.*, Nature (London) **452**, 970 (2008); D. Hsieh *et al.*, Science **323**, 919 (2009).
- [26] J.D. Sau, *et al.*, arXiv:0907.2239.